Characterization of Dnajc12 knockout mice, a model of hypodopaminergia

Authors

Isaac Bul Deng[1], Jordan Follett[1], Jesse D. Fox[2] and Matthew J. Farrer[1*]

[1]Department of Neurology, and Norman Fixel Institute for Neurological Diseases, University of Florida, Gainesville, Florida, USA.

[2]Department of Medical Genetics, University of British Columbia, Vancouver, BC, Canada.

***Corresponding author:** Matthew J. Farrer (email: m.farrer@ufl.edu)

Word count: 5,355 including figure legends

Figures: 6

Tables:0

Supplementary figures: 4

Abstract

Homozygous *DNAJC12* c.79-2A>G (p. V27Wfs*14) loss-of-function mutations were first reported as a cause of young-onset Parkinson's disease. However, bi-allelic autosomal recessive pathogenic variants in *DNAJC12* may lead to an alternative constellation of neurological features including infantile dystonia, developmental delay, intellectual disability and neuropsychiatric disorders. DNAJC12 is understood to co-chaperone aromatic amino acid hydroxylases to enhance the synthesis of biogenic amines. *In vitro*, we confirm overexpressed DNAJC12 forms a complex with tyrosine hydroxylase, the rate-limiting enzyme in dopamine (DA) synthesis. Now we describe a conditional knockout mouse (cDKO) in which loxP sites flanking *Dnajc12* exon 2 enable its excision by cre-recombinase to create a constitutive *Dnajc12* knock out (DKO). At three months of age, DKO animals exhibit reduced locomotion and exploratory behavior in automated open-field testing. DKO mice also manifest increased plasma phenylalanine levels, a cardinal feature of patients with *DNAJC12* pathogenic variants. In striatal tissue, total DA and serotonin, and their metabolites, are reduced. Biochemical alterations in synaptic proteins and tyrosine hydroxylase are also apparent, with enhanced phosphorylation of pSer31 and pSer40 sites that may reflect biological compensation. Electrically-evoked striatal DA is reduced. Most immediately, cDKO and DKO mice present models to develop and refined therapeutic approaches for the treatment of DNAJC12 dystonia and parkinsonism. These models may also enable the pleiotropic functions of biogenic amines (including DA) to be individually investigated in the brain and periphery.

Introduction

A major pathological hallmark of neurodegenerative diseases is the presence of intracellular and extracellular protein inclusions, indicative of altered proteostasis.[1,2] The maintenance of cellular proteome requires molecular chaperones known as heat shock proteins (HSP), which comprise HSP90, HSP70, HSP60, HSP40 and small HSPs. This diverse superfamily has a fundamental role in protein folding, trafficking and degradation.[1,2]Biallelic, recessively inherited pathogenic variants in *DNAJC12*, a member of the DNAJC family, also referred to as HSP40, induce a multitude of neurological disorders, including young-onset parkinsonism, infantile dystonia, developmental delay, intellectual disability and neuropsychiatric disorders.[3–9] Variants in *DNAJC12* also account for a small proportion of cases of hyperphenylalaninemia (HPA), which is prominently attributed to variants in phenylalanine hydroxylase (PAH), and its cofactor tetrahydrobiopterin (BH_4).[4,5,9,10]Although its function has yet to be fully understood, DNAJC12 is widely regarded as a co-chaperone for aromatic amino acid hydroxylases (AAAHs) including PAH, tyrosine hydroxylase (TH) and tryptophan hydroxylase 1 and 2 (TPH1 and TPH2).[3,4] Patients with *DNAJC12* variants have reduced levels of dopamine (DA) and serotonin (5-HT) metabolites in their cerebrospinal fluid, congruent with the role of DNAJC12 as a co-chaperone for TH and TPH2, respectively.[3–6,9]

Besides DNAJC12, several members of the DNAJC family of co-chaperones are implicated in parkinsonism including cysteine string protein-α (DNAJC5), auxilin (DNAJC6), receptor-mediated endocytosis-8 (DNAJC13) and cyclic G associated kinase (DNAJC26).[11–14] We have similarly identified heterozygous mutations in guanosine triphosphate (GTP) cyclohydrolase I (GCH1), the rate-limiting step in the conversion of GTP to tetrahydrobiopterin (BH_4), in patients with postural dystonia in childhood that becomes generalized [15,16] or with late-onset Parkinson's disease (PD).[17–19]Although these movement disorders are considered phenotypically, physiologically and molecularly distinct, both occur within different individuals of the same families, with the same

mutations, within genes in intersecting pathways. What underlies this profound difference in penetrance and presentation remains enigmatic.[20] Clearly, dystonia and/or parkinsonism in patients with *DNAJC12*[3–5,21,22] or *GCH1*[15,18,23,24] pathogenic variants can be attributed to DA dysregulation as each is responsive to DA-replacement therapy (levodopa (L-DOPA) treatment). Thus, understanding the role of DNAJC12 in DA synthesis may reveal novel strategies to re-establish DA levels, which could help to alleviate dystonia and parkinsonism, emphasizing the importance of establishing *in-vivo Dnajc12* models. The first homozygous pathogenic variant discovered in human disease was *DNAJC12* c.79-2A>G (p. V27Wfs*14), which results in exon 2 skipping and nonsense-mediated decay.[5] In the murine sequence, exon 2 deletion alters the open reading frame after amino acid 26 (exon 1), and is predicted to result in 44 novel amino acids that terminate in a stop mutation (p. V27Wfs*44). Primarily, exons 2 and 3 encode the DNAJC and Hsp70 interaction domains. We have generated murine Dnajc12 knockout mice (Dnjac12 p. V27Wfs*44) and have used these mice to characterize the role of Dnajc12 in DA synthesis, physiology and related behavior.

Methods

Animals

All animal procedures were performed in accordance with the protocol approved by the Institutional Animal Care and Use Committee of the University of Florida. We generated a *Dnajc12* knockout (DKO) mouse model on a C57BL/6J background with Jackson Laboratories. CRISPR/Cas9 editing was used to insert a pair of loxP sites flanking exon 2 to create a conditional allele and a mouse strain (cDKO). Cre recombination was then used to ablate the intervening sequence with a germline cre transgenic cross. The gene locus for murine *Dnajc12* is on chromosome 10 at 63,218,222-63,244,619 (GRCm39: GCF_000001635.27). The main protein encoding isoform 1 encodes 198 amino acids and is denoted by NCBI transcript RefSeq ID NM_013888.3. It comprises 5 exons that generate a mRNA of 1305bp. There is a second shorter

isoform 2 (NM_001253685.1) that uses a different exon 1, which is predicted to encode 116 amino acids but lacks a DNAJC domain. The first homozygous mutation discovered in human disease was *DNAJC12* c.79-2A>G (p.V27Wfs*14), that results in exon 2 skipping and nonsense-mediated decay.[5] Exon 2 deletion in the murine sequence (ENSMUSE00001301217, Chr10:63,231,564-63,231,642 [GRCm39]) also alters the open reading frame after amino acid 26 (exon 1) and is predicted to result in 44 novel amino acids that terminate in a stop mutation (p. V27Wfs*44). The DKO mice were maintained by heterozyous breeding on a reverse light cycle (from 8 pm to 8 am) and single-sex group-housed in enrichment cages after weaning at post-natal day 21. All mice were supplied with a standard rodent chow and water *ad libitum*. Ear notches were taken at *post-mortem* for post-hoc genotyping with the following primer sequences 5'-CCAGGCCTGGCTTTTATTTG-3' and 5'-TTAAGTCCAAACCAGCTGCC-3' using standard thermocycling conditions. All experiments, data processing and analysis were conducted in a blinded manner.

Behavior

Open field test: The Activity Monitor System uses an array of infrared (IR) photo beams to measure locomotion and motor activity in a square open field arena with a duration of 30 min. The apparatus consists of 3 sets of matching IR photo beams that project across the open field along x, y and z axes. The software detects when and where photo beams are disrupted by an animal. The software also allows the open field arena to be broken into zones or areas of interest depending on the experiment, and data analysis displays the measurements accordingly.[25]

Grip Strength test: Neuromuscular function and muscular strength was assessed by measuring the peak force required to make the animal release its grip.[26] The Grip Strength test apparatus consists of a baseplate, a trapezoidal stainless-steel grip, and a force sensor. To measure grip

strength, mice are gently lifted by the tail such that the fore paws or hind paws can grasp onto the steel grip, and then gently pulled away from the apparatus by the tail until they release their grip.

Balance beam: Sensorineural balance and coordination was examined by placing mice on an elevated narrow square beam of 100 cm in length, with an enclosed dark platform at the end of the beam.[27,28] Mice are trained on a beam of 24 mm in width and then tested on a 12 mm. Videos are recorded from both sides of the beam, and total foot slips are measured.

Antibodies: Rabbit monoclonal or polyclonal antibodies include those against 14-3-3 (Invitrogen, 51-0700, 1:1000); clathrin heavy chain (Abcam, ab21679, 1:1000); DNAJC5 (Synaptic systems, 154003, 1:1000); DNAJC12 (12338-1-AP, Proteintech; 1:1000); Endophilin 1 (Synaptic systems, 159002, 1:2000); GFP (Abcam, ab290; 1,10,000); HSC70 (Abcam, ab51052; 1:1000); myelin basic protein (Abcam, ab218011, 1:1000); olig2 (Abcam, ab109186, 1:1000); Synaptobrevin 2 (VAMP2) (Synaptic systems, 104202, 1:1000); tyrosine hydroxylase (pser40) (Sigma, T9573, 1:1000); tyrosine hydroxylase (pSer31) (Sigma, SAB4300674, 1:1000); β-tubulin (Abcam, ab6046; 1:4000). Mouse monoclonal antibodies include those raised against: GAPDH (ThermoFisher Scientific, MA5-15738; 1:5000), FLAG (M2 clone, Millipore-Sigma, F3165; 1:5000); tyrosine hydroxylase (TH) (Sigma, T2928, 1:1000); SNAP25 (Synaptic systems, 111011, 1:1000).

Tissue collection and homogenization: Mice were deeply anaesthetized via inhalation of isoflurane and then intracardially perfused with phosphate buffer saline (PBS) prior to microdissection of the midbrain and striatum. For analysis of total protein, micro-dissected tissues were homogenized at 20% w/v in 1x Cell Signaling Lysis Buffer (#9803S) with 1x Halt™ Protease and Phosphatase Inhibitor Cocktail (Thermofisher #78442) using a 1 mL glass Dounce

homogenizer (Wheaton) and placed on ice for 30 min before being cleared by centrifugation (14,000 g at 4ºC for 20 min). The total protein concentration in the supernatant was measured with BCA assay (Pierce).[29,30]

Cell culture: HEK293FT (Thermofisher Scientific; R70007) cell line was maintained in high glucose Dulbecco's Modified Eagles Medium (DMEM), respectively, supplemented with 10% (v/v) FBS (Gibco), 2 mM l-glutamine (Thermo Fisher Scientific) and penicillin/streptomycin. Cultures were maintained in 5% CO2 at 37 °C.[31] Transient transfection of cDNA was performed by using Lipofectamine 2000 (Thermo Fisher Scientific), while siRNA was transfected using Lipofectamine RNAiMAX (Thermofisher Scientific) according to the manufacturer's instruction.

Co-immunoprecipitation: For experiments where epitope-tagged constructs were transiently overexpressed, HEK293 cells were seeded in 10 cm dishes and transfected with the indicated plasmids. At 48h post-transfection, cells were washed once in ice-cold PBS and lysed in 1 mL of Cell lysis buffer (Cell signaling #9803S) supplemented with 1x Halt™ Protease and Phosphatase Inhibitor Cocktail (Thermofisher #78442) and incubated on ice for 30 min with gentle agitation every 15 min before being cleared by centrifugation at 14, 000 ×g for 12 min at 4°C. 20 µL of cleared lysate was collected as input, and GFP was recovered from the lysate using 20 µL of pre-equilibrated GFP-Trap (gta-20, ChromoTek) for 1h at 4 °C. Beads were collected by centrifugation and washed 4-6 times with 1 mL of lysis buffer followed by centrifugation before elution (10 min, 90 °C) in 2 x SDS-loading buffer prior to standard SDS-PAGE and western blotting.

SDS-PAGE and Western blotting: 20-40 µg of denatured lysates were resolved by SDS-PAGE on 4-20% TGX Criterion TGX pre-cast gels (Bio-rad) and transferred to nitrocellulose membranes by semi-dry trans-Blot Turbo transfer system (Bio-rad). The membranes were blocked with either 50% Intercept tris buffered saline (TBS) Blocking Buffer (927-60001), 5% bovine serum albumin

(BSA) in TBS-Tween (TBST), or 5% milk in TBST for 1h at room temperature (RT) followed by incubation overnight with primary antibodies diluted in blocking buffer at 4°C. After incubation with primary antibodies, the membranes were washed in TBST (3 x 5 min), followed by incubation for 1h at RT with fluorescently conjugated goat anti-mouse or rabbit IR Dye 680 or 800 antibodies (Licor). The blots were washed in TBST (3 x 10 min) and scanned on a ChemiDoc MP imaging platform (Bio-Rad).[29,30]

Immunofluorescence with confocal microscopy: For imaging of Dnajc12 in the *SNpc*, 3M old WT mice were anesthetized via intraperitoneal administration of sodium pentobarbital (240 mg/kg, i.p.), and intracardially perfused with PBS then 4% paraformaldehyde (PFA) in PBS. Brains were extracted, post-fixed overnight at 4°C in 4% PFA, then cryoprotected with an increasing sucrose gradient (10%, 20%, 30% in PBS) overnight at 4°C. Coronal slices (30 µm) were obtained by cryostat. Sections were block in 10% normal goat serum (NGS) in 0.3% PBST (1h, 37^0), followed by incubation of primary antibodies: rabbit anti-DNAJC12 (12338-1-AP, Proteintech; 1:200) and chicken anti-TH (ab76442 Abcam; 1:1000) made in antibody solution (5% NGS + 0.1% PBST) overnight at 4°C. The sections were washed (4x15 min in PBST), followed by secondary antibody incubation with species-specific Alexafluor IgG secondary antibodies (90 min at RT, Invitrogen; 1:1000). Tissues were washed again in 0.1% PBST (4 x 15 min), then mounted using DAPI Fluoromount-G® (0100-20, SouthernBiotech). Images were acquired using a 60x oil objective on an Olympus Fluoview FV-1000 confocal laser scanning microscope (9 x 0.33µm step size). Images were stacked (three stacks of 3 individual images viewing 1µm tissue depths) using FIJI ImageJ software (NIH, USA).

Electrophysiology: Fast scan cyclic voltammetry (FSCV) was used to assess evoked dopamine release and reuptake in 300 µm hemi-coronal slices of the dorsolateral striatum, as previous.[29,30] Coronal striatal slices obtained from 3M DKO mice with a vibratome were perfused with

oxygenated artificial cerebrospinal fluid (aCSF) at RT for ~1h prior to experiments. Stimuli are delivered by nickel-chromium bipolar electrodes (made in house) placed in the dorsolateral striatum, optically isolated (World Precision Instruments, USA) and controlled/sequenced with ClampEx software. Voltammetric responses were recorded, standardized and analyzed with an Invilog Voltammetry system and software (Invilog), using carbon fiber electrodes (diameter: 32μm, length: 30μm, sensitivity: 21-40nA/μM; Invilog) and placed within 100-200 μm of the stimulating electrode in the dorsolateral striatum. Field activity was recorded to ensure the viability of the slice during the recording. Input/output paradigms were as previous.[32,33] At the end of each recording session, a three-point calibration of each carbon fiber electrode is conducted (final concentrations of DA in a CSF (μM): 0.5,1.0 and 2).

High-performance liquid chromatography (HPLC). Sample preparation and HPLC were performed by the Emory HPLC Bioanalytical Core (EHBC) according to their protocol. In brief, striatal tissues were suspended in 300 μL solution of 0.1M PCA and 0.1mM EDTA, followed by sonication, then centrifugation of the homogenates at 10,000 x g for 15 min at 4°C to obtain the supernatant. The concentration of DA,5-HT and their metabolites in the supernatant were determined by reverse phase HPLC with electrochemical detection using an ESA 5600A CoulArray detection system equipped with an ESA Model 584 pump and an ESA 542 refrigerated autosampler.

Metabolomics: Plasma samples for DKO and WT mice were sent to Creative Proteomics to analyze free amino acids and related metabolites, which was conducted per their protocol. To summarize, 20 μL of each plasma sample was added into an Eppendorf tube containing 80 μL of the internal standard solution (contains 41 isotope-labeled internal standards). The resultant mixture was sonicated for 5 min and centrifuged at 21,000 x g for 10 min before taking the supernatant. 50 μL of supernatant for each sample or the standard calibration solution was mixed

with 100 µL of 20 mM dansyl chloride solution and 100 µL of borate buffer (pH 9), and allowed to react for 30 min at 40°c. Aliquots of the resultant solutions (5 µL) were injected to run UPLC-MRM/MS on a Waters Acquity UPLC system coupled to a Sciex QTRAP 6500 Plus mass spectrometer equipped with a heated ESI source. LC separation was carried out on a C18 UPLC column (2.1*150 mm, 1.8 µm) with 0.1% formic acid in water and 0.1% formic acid in an acetonitrile-isopropanol mixed solvent as the binary-solvent mobile phase for gradient elution (20% to 90% B in 20 min), at 55 °C and 0.3 mL/min.

Statistical analysis: The data for the automated open field test was acquired with Activity Monitor 7 software (Med Associates Inc), and for the grip test, the data acquisition and extraction of the spike corresponding to the force exerted by the subjects was analyzed with Grip Strength Software (Maze Engineers). The DA traces for FSCV were analyzed with Clampfit (Molecular devices), and the densitometric analyses were performed with Image J software. Normality testing and statistical analysis of all the data were performed using GraphPad Prism 10. The data is presented as mean ± standard error of the mean (SEM).

Results

Identification of DNAJC12 interacting partners *in-vitro*

Recently, unbiased mass-spectrometry in HEK293 cells overexpressing the co-chaperone DNAJC12 revealed its interaction with DA synthesizing enzyme, tyrosine hydroxylase (murine 'Th', human 'TH').[4] To build upon this data, HEK293 cells transiently co-transfected with combinations of epitope-tagged *DNAJC12* and *TH* (GFP-DNAJC12 and FLAG-TH) were lysed and lysates immunoprecipitated with GFP-agarose beads. GFP-tagged DNAJC12 co-immunoprecipitated FLAG-TH and endogenous HSC70 while empty vector GFP control did not (Fig 1), consistent with recent mass-spectrometry findings.[4] To confirm this interaction is not limited to overexpression systems, lysates generated from sub-cortical brain tissue of wildtype

mice (WT) were immunoprecipitated with anti-Th antibody-coated beads then eluted and subjected to Western blot (WB) analysis, with complementary findings as in Fig S1a. Also, we used fluorescence immunohistochemistry (IHC) with confocal microscopy to visualize the sub-cellular localization of Dnajc12 within Th-positive neurons in midbrain slices from WT animals. Dnajc12 fluorescent puncta were observed within the soma, dendrites and axons of Th positive dopaminergic (DA) neurons in the midbrain (Fig.1Sb).

3M DKO mice have impaired locomotion and exploratory behavior in the automated open field test. CRISPR/Cas9 editing was used to insert a pair of loxP sites on either side of exon 2 of murine *Dnajc12*, followed by cre-mediated excision to generate a constitutive knockout of *Dnajc12* (DKO mice) (Fig 2a**)** as detailed in methods*.* Our major focus is to investigate the effects of Dnajc12 ablation in nigrostriatal DA synthesis, physiology and behavior, given individuals with pathogenic variants in *DNAJC12* response so well to DA-replacement therapy. Thus, we successfully confirmed the ablation of *Dnajc12* with genomic PCR (Fig 2b) and loss of protein expression in the striatum and midbrain (Fig 2c-e). We proceeded to characterize the behavior of these mice at 3M, relative to WT littermates, using an automated open field test; DKO mice had a significant reduction in their ambulatory distance (Fig 3b), ambulatory time (Fig 3c), number of rears (Fig 3e) and average speed (Fig 3f), along with an increase in resting time (Fig 3d), all of which are indicative of impaired locomotion/exploratory behavior. There were no deficits in grip strength **(**Fig 3g) or motor coordination (Fig 3h-i) based on the grip test and beam, respectively.

Th protein level and its phosphorylated residues are altered in the midbrain and striatum of DKO mice. As DNAJC12 is an essential co-chaperone for TH,[34] we examined the effect of its loss on Th levels and phosphorylation state in midbrain (where DA neuron cell bodies reside) and striatum (location of their terminals). Additionally, we assessed the expression of heat shock

cognate 70 (Hsc70) and 14-3-3, which are implicated in DA biosynthesis. Hsc70 is reported to interact with vesicular monoamine transporter (VMAT2), TH and aromatic amino acid decarboxylase (AADC), indicating its importance in DA synthesis.[35,36] Similarly, 14-3-3 may modulate the degree of activation of TH by regulating its phosphorylation.[37] The protein expression of Hsc70 and 14-3-3 in the midbrain and striatum (Fig 4b-c, h-i) was comparable between DKO mice and WT littermates as well as the total Th levels in the striatum (Fig 4d). However, the phosphorylation at the pSer40 site was significantly increased, while pSer31 was reduced (Fig 4e-f) in the striatum in the DKO compared to WT. In contrast, total Th, pSer31 and pSer40 were all elevated in the midbrain (Fig 4j-l).

DKO mice have reduced striatal DA and peak response

DA neurons in the *substantia nigra par compacta* (*SNpc,* located in the midbrain) extend their axons via the medial forebrain bundle to the striatum, where DA is released as a volumetric neuromodulator of synaptic transmission.[38] We micro-dissected the striatum to measure DA levels with HPLC. Striatal DA (43.70 versus 58.86 ng/mg), and its metabolites 3,4 - dihydroxyphenylacetic acid (DOPAC) (3.20 versus 5.62 ng/mg) and homovanillic acid (HVA) (4.052 versus 6.823 ng/mg) were markedly reduced in DKO mice compared to their WT littermates (Fig 5a-c). Also, DKO mice exhibit reduced levels of striatal 5-HT (Fig S2 a-c) and increased plasma levels of phenylalanine (Phe) (Fig S3a). However, other amino acids, such as tyrosine (Tyr) and tryptophan (Trp) (Fig S3 b-c), were unchanged. Reduced striatal 5-HT coincides with the role of Dnajc12 as a co-chaperone for TPH2, the rate-limiting enzyme in the synthesis of 5-HT in the central nervous system, while increased Phe levels denote the role of Dnajc12 as a co-chaperone for PAH, which catalyzes the conversion of Phe into tyrosine, an essential amino acid required for DA synthesis. Interestingly, loss of Dnajc12 didn't change the levels of plasma biogenic amines as measured with mass-spectrometry (Fig S3 d-g). To examine changes in striatal DA dynamic, we measured DA release and reuptake in *ex-vivo* striatal slices

with FSCV (Fig 5e-g). When electrically stimulated, slices from DKO mice had a significantly lower peak response compared to WT mice (0.140 versus 0.30 μM) (Fig 5h), which reconciles with reduced striatal DA levels. The decay constant tau was comparable between DKO and WT mice (415 versus 425 ms) (Fig 5i), indicating no alteration in the reuptake kinetics of DA at the terminals.

Expression of synaptic proteins is altered in the striatum of 3M old Dnajc12 mice.

DNAJC12 interacts with VMAT2, AADC and HSC70, making it central in DA synthesis.[35,36] However, loss of Dnajc12 could alter other synaptic proteins involved in DA neurotransmission. Thus, we examine the expression of striatal synaptic proteins, including other DNAJC family of proteins implicated in parkinsonism. There were no changes in proteins such as clathrin heavy chain (Chc) (Fig 6b), vesicular associated membrane protein 2 (Vamp2) (Fig 6e), and cysteine string protein-α (Dnajc5) (Fig 6f). In contrast, synaptosomal associated protein 25 (Snap25) (Fig 6d) was significantly reduced while endophilin 1A (Fig 6c) was increased in DKO mice compared to WT.

Discussion

DA deficiency is a core feature of patients with *DNAJC12* mutations, congruent with this protein's role as a co-chaperone for the DA synthesizing enzyme TH.[3–5] Earlier studies with unbiased mass-spectrometry in HEK293 cells overexpressing DNAJC12 revealed its interaction with TH, which we confirmed *in-vitro* by co-immunoprecipitation in HEK293 cells transiently co-transfected with GFP-tagged DNAJC12 and FLAG-TH. Consistent with immunoaffinity-mass spectrometry in cells expressing epitope-tagged DNAJC12[39], we confirmed DNAJC12 co-immunoprecipitated Hsc70 in HEK293 cells, which may influence DA biosynthesis and packaging indirectly via its interaction with VMAT2, TH and AADC.[35,36]DA is critical in regulating movement, attention, addiction, reward, cognition, arousal, wakefulness and cognition.[40–42] These functions are under

the control of dopaminergic circuits, which include the nigrostriatal, mesocortical and mesolimbic pathways.[40]We reason that deficits in the DA system are responsible for many (but not all) of the neurological problems observed in patients with *DNAJC12* mutations.[5,6,8,43,44] Hence, we aimed to assess the effects of loss of Dnajc12 on DA biology, physiology and behavior. The DKO mice carry Dnajc12 p. V27Wfs*44, which resembles the *DNAJC12* c.79-2A>G (p. V27Wfs*14), the first homozygous pathogenic variant discovered in patients with young-onset parkinsonism. In humans and mouse, skipping of exon 2 results in nonsense-mediated decay.

Comparative analyses in 3M DKO and WT littermates indicate that DKO exhibits a reduction in locomotion and exploratory behavior as shown by their ambulatory distance, ambulatory time, number of rears, average speeds and resting time in the automated open field testing. However, there are no definitive motor deficits, as signified by grip test and beam, which assess grip strength and motor coordination, respectively. Motor deficits in patients with pathogenic variants in *DNAJC12* are often preceded by neurodevelopmental and neuropsychiatric features, which may coincide with reduced exploratory/locomotion in DKO mice without motor deficits. Additional behavioral tests such as elevated-plus maze for anxiety-like behavior or Bussey Sakada boxes for cognition in 3M DKO mice may complement the early behaviour phenotype. Our major focus was to investigate the effects of Dnajc12 ablation on nigrostriatal DA synthesis since Dnajc12 is a prominent co-chaperone for Th. We micro-dissected the midbrain and striatum to assess Th protein expression and its phosphorylation. The total Th, pSer31 and pSer40 were all elevated in the midbrain, while only pSer40 was increased in the striatum in DKO compared to WT. TH phosphorylation at its serine residues correlates with its activity[45]; therefore, these findings reflect potential compensation in Th activity to meet the demands of DA synthesis due to the loss of Dnajc12. Also, 3M DKO have reduced levels of striatal DA and its metabolites DOPAC and HVA. These findings are consistent with reduced peak response amplitude when DA release is evoked electrically in *ex-vivo* striatal slices. Synaptic proteins involved in neurotransmission either via the

formation or release of synaptic vesicles, such as endophilin 1 and SNAP25 were also altered in DKO mice. Collectively, these findings indicate that loss of Dnajc12 may alter interaction, stability and activity of Th, culminating in reduced DA levels and behavioral deficits. In PD, the degeneration of DA neurons in the midbrain is accompanied by reduced TH protein/activity in the remaining neurons.[46–48] The WB results for expression of TH in the striatum and midbrain imply that the nigrostriatal DA neurons remain intact at 3M of age. However, loss of Dnajc12 in DA neurons might induce a variety of compensation strategies (including enzymatic, energetic, intra-/extracellular and morphologic changes) to enhance endogenous dopaminergic innervation that, nevertheless, may become pathophysiologic adaptations with age, fostering DA neuron degeneration.

It is important to note that DKO mice have reduced levels of striatal 5-HT, supporting the role of Dnajc12 in the synthesis of other biogenic amines. Interestingly, the plasma biogenic amines were comparable between DKO and WT. 5-HT in the periphery has a role in gastrointestinal motility and inflammation, while the catecholamines (including DA, adrenaline and noradrenaline) are essential in autonomic response, whereby they are secreted into the bloodstream as hormones with significant effects on many peripheral organs. Thus, changes in peripheral biogenic amines in DKO mice may be evoked under specific stimuli. Furthermore, DKO mice have increased levels of plasma Phe, a cardinal feature in human patients with similar pathogenic DNAJC12 variants, supporting the role of Dnajc12 as co-chaperone for PAH, which converts Phe to tyrosine, required for DA synthesis. Therefore, the specific dopaminergic effects in DKO mice can be confounded by the concomitant deficits in other AAAHs, which can be remedied using specific adeno-associated virus (AAV) in conditional floxed cDKO mice to ablate Dnajc12 in DA neurons.

For the first time, we characterize the DKO mice, which manifest reduced locomotion/exploratory behavior and biogenic amines levels, with concomitant mild HPA, which recapitulate *DNAJC12*

mutations in human disease. Parkinsonism and/or dystonia in patients with *DNAJC12*[3–5,21,22] or *GCH1*[15,18,23,24] mutations can be attributed to DA dysregulation as each is responsive to L-DOPA treatment. Therefore, DKO is a suitable preclinical model to ascertain the pathobiology and uncover therapeutic strategies for the aforementioned disorders. Moreover, any therapeutic approach to increase TH protein/activity or DA synthesis is likely to be beneficial for a wide range of neurological disorders of dopamine neurotransmission. Interestingly, BH_4 appears to modulate TH expression and its activity.[46,49] Studies in PD report reduced BH_4 concentration and GCH1 activity in the *substantia nigra* and striatum and low BH_4 levels in cerebrospinal fluid (CSF).[46,50] However, preclinical experiments with BH_4 have yet to prove conclusive. Some studies suggest an increased level of BH_4 is toxic to catecholamine cells[51], while others indicate increased levels of BH_4 will stimulate TH activity and DA release. Thus, DKO mice are also invaluable to investigate the mechanism and therapeutic effects of BH4 *in-vivo*, which can be useful as a preventative/treatment option for individuals with dopaminergic dysfunction.

Figure legends:

Fig 1. DNAJC12 co-immunoprecipitated TH and Hsc70 in HEK293 cells. HEK293 cells transiently co-transfected with combinations of epitope-tagged *DNAJC12* and *TH* (GFP-DNAJC12 and FLAG-TH) were lysed and lysates immunoprecipitated with GFP-agarose beads 48 hr post-transfection. The lysates were then resolved with SDS-page and probed with the respective antibodies.

Fig 2. Depiction of *Dnajc12* ablation in 3M old DKO mice. Illustration of cre-mediated excision of *Dnajc12 (**a**).* Genomic PCR for *Dnajc12* (**b**). Representative blots for Dnajc12 expression in the midbrain (MB) and striatum (STR) (**c**). Densitometric analyses of Dnajc12 expression in the MB (**d**, unpaired *t*-test, $t_{11} = 16.69$, $p < 0.0001$) and striatum (**e**, unpaired *t*-test, $t_{10} = 7.798$, $p < 0.0001$). ****$p < 0.0001$. *Error bars are* ± *SEM.* WT n =4-5, DKO n = 8.

Fig 3. *Dnajc12* ablation impairs locomotion and exploratory behavior in the automated open field in 3M old DKO mice. **a**) The weight of WT and DKO mice is comparable (Unpaired *t*-test with Welch's correction, $t_{22.74} = 0.53$, $p = 0.60$). DKO mice have a significant reduction in their ambulatory distance (**b**, Unpaired *t*-test with Welch's correction, $t_{23.16} = 2.58$, $p = 0.02$), ambulatory time (**c,** Unpaired *t*-test, $t_{32} = 2.62$, $p = 0.01$), number of rears (**e,** Unpaired *t*-test, $t_{32} = 4.29$**,** $p = 0.0002$) and average speed (**f**, Unpaired *t*-test, $t_{32} = 2.58$, $p = 0.01$), along with increased resting time (**d,** Unpaired *t*-test, $t_{32} = 2.78$, $p = 0.001$), all of which are indicative of impaired locomotion/exploratory behavior. Grip strength (**g,** Unpaired *t*-test, $t_{32} = 0.46$, $p = 0.65$) and sensorineural balance and coordination were comparable between WT and DKO (**h,** Unpaired *t*-test, $t_{32} = 0.26$, $p = 0.80$; **i**, Unpaired *t*-test, $t_{31} = 0.54$, $p = 0.59$). **p < 0.05, **p < 0.01, ***p < 0.001. Error bars are* ± *SEM.* 3M old mice, WT n = 16, DKO n = 18.

Fig 4. 3M DKO mice exhibit alterations in Th protein, and its phosphorylated species in midbrain (MB) and striatum (STR). Representative blots for the STR and MB (**a, g**). The expression of Hsc70 (**b**, Unpaired *t*-test, $t_{19} = 1.41$, $p = 0.17$), 14-3-3 (**c,** Unpaired *t*-test, $t_{19} = 1.57$, $p = 0.13$) and tTh (**d**, Unpaired *t*-test with Welch's correction, $t_{16.68} = 0.26$, $p = 0.79$) in the striatum was comparable between WT and DKO mice. In contrast, pSer31 (**e**, Unpaired *t*-test, $t_{18} = 4.52$, $p = 0.0003$) was significantly reduced while pSer40 was increased (**f**, Unpaired *t*-test, $t_{19} = 3.93$, $p = 0.0009$). The expression of Hsc70 (**h**, Unpaired *t*-test, $t_{16} = 0.43$, $p = 0.67$) and 14-3-3 (**i**, Unpaired *t*-test, $t_{16} = 1.76$, $p = 0.09$) was not altered in the midbrain in WT compared to DKO, meanwhile tTh (**j**, Unpaired *t*-test, $t_{16} = 2.64$, $p = 0.01$), Th pSer31 (**k**, Unpaired *t*-test with Welch's correction, $t_{14} = 2.332$, $p = 0.04$) and Th pSer40 (**l**, Unpaired *t*-test, $t_{18} = 2.70$, $p = 0.01$) were significantly increased. **p < 0.05, ***p < 0.001. Error bars are* ± *SEM.* 3M old mice, WT n= 8-9, DKO n = 10-12.

Fig 5. Dnajc12 knockout reduces the levels of striatal DA, and its metabolites, and the peak amplitude of its release in 3M DKO mice. a) Depiction of DA metabolism. Levels of DA (**b,** Unpaired *t*-test, t_{24} = 2.25, p =0.03**)**, DOPAC (**c,** Unpaired *t*-test with Welch's correction**,** $t_{15.43}$ = 4.01, p = 0.001) and HVA (**d,** Unpaired *t*-test with Welch's correction, $t_{17.36}$ = 3.74, p = 0.002) via HPLC (WT n = 13, DKO n = 13). **e**) Depiction of the electrode's placement into the striatal slices, n refers to the number of mice and in the parentheses the number of slices (WT n = 5 (20); DKO n = 4 (16)). Representative DA traces for WT and DKO (**f**). A series of increasing intensity single pulse stimuli were delivered every 2 min, and the input – output peak response is as indicated (**g,** starting for 100 to 500 μA, 2-way ANOVA with Šídák's multiple comparisons test: t_{29} = 4.14, p = 0.001; t_{29} = 3.54, p = 0.007; t_{29} = 3.62, p = 0.006; t_{29} = 4.10, p = 0.002; t_{29} = 5.43, p = <0.0001). Single pulse peak response (stimulation at 400 μA) with 70% of the maximum DA release (**h,** Unpaired *t*-test, t_{34} = 8.23, p <0.0001). Single pulse tau (ms) (**i**, Unpaired *t*-test, t_{33} = 0.13, p = 0.90). **p < 0.05, **p < 0.01, ****p < 0.0001. Error bars are ± SEM.*

Fig 6. Dnajc12 knockout on the expression of synaptic proteins in the striatum (STR). Representative blots for the expression of synaptic proteins in the striatum (STR) (**a**). Densitometric analyses for clathrin heavy chain (Chc) (**b**, *Unpaired t*-test, t_{19} = 0.07, p = 0.94), endophilin 1 (**c**, Unpaired *t*-test with Welch's correction, $t_{11.20}$ = 2.70, p = 0.02), synaptosomal associated protein 25 (Snap-25) (**d**, *Unpaired t*-test, t_{18} = 2.35, p = 0.03), vesicular associated membrane protein 2 (Vamp2) (**e**, *Unpaired t*-test, t_{19} = 1.34, p = 0.19) and cysteine string protein-α (Dnajc5) (**f**, *Unpaired t*-test,t_{19} = 0.20, p = 0.84). **p < 0.05. Error bars are ± SEM.* 3M old mice, WT n= 9, DKO n = 12).

Supplementary figure legends:

Fig S1. Dnajc12 which interacts with Th *in-vivo* localizes to the soma, dendrites and axons in Th-positive neurons. a) Co-immunoprecipitation assay depicting Dnajc12 interaction with Th. **b**) Immunofluorescent labelling with confocal microscopy showing Dnajc12 puncta in the soma, dendrites and axons in Th-positive neurons in coronal slices obtained from WT C57BL/6 mice.

Fig S2. Striatal serotonin (5-HT) levels and its metabolite are reduced in 3M DKO mice. Depiction of serotonin synthesis pathway (**a**). Levels of 5-HT (**b**, Unpaired *t*-test with Welch's correction, $t_{17.36} = 3.74$, $p = 0.002$) and its metabolite 5-HIAA (**c**, Unpaired *t*-test with Welch's correction, $t_{13.06} = 6.85$, $p < 0.001$). **$p < 0.01$, ***$p < 0.001$. Error bars are ±SEM. (WT n = 13; DKO n=13).

Fig S3. Dnajc12 knockout recapitulates hyperphenylalaninemia as exemplified in human patients with similar pathogenic variants, but doesn't alter plasma biogenic amines. Levels of plasma phenylalanine (Phe) (**a,** Mann-Whitney test, $p = 0.005$), tyrosine (Tyr) (**b,** Mann-Whitney test, $p = 0.47$), tryptophan (Trp) (Mann-Whitney test, $p = 0.41$) and plasma biogenic amines which include DA (**d**, Mann-Whitney test, $p = 0.31$), NE (Mann-Whitney test, $p = 0.18$), Adrenaline (**f**, Mann-Whitney test, $p > 0.10$) and 5-HT (**g**, Mann-Whitney test, $p = 0.84$). **$p < 0.01$. Error bars are ±SEM. 6-8M old mice, WT n=9, DKO n=7.

Fig S4. Oligodendroglial markers are unchanged in the striatum (STR) and midbrain (MB) of 3M DKO mice. Representative blots for MBP and Olig2 in the STR (**a)** and MB (**d**). Densitometric analysis of MBP-STR (**b**, Unpaired *t*-test with Welch's correction, $t_{10.16} = 1.14$, $p = 0.28$), Olig2 – STR (**c**, unpaired *t*-test, $t_{19} = 0.72$, $p = 0.48$), MBP-MB (**e**, Unpaired *t*-test with Welch's correction, $t_{10.75} = 1.27$, $p = 0.23$) and Olig2-MB (**f**, unpaired *t*-test, $t_{19} = 0.06$, $p = 0.96$). Error bars are ±SEM. (WT n = 9; DKO n=12).

Acknowledgement. This study was supported in part by the Emory HPLC Bioanalytical Core (EHBC), which was supported by Emory University School of Medicine and the Georgia Clinical & Translational Science Alliance of the National Institutes of Health under Award Number UL1TR002378.

Author contribution: IBD: conceptualization and project design, data curation, formal analysis, writing original draft, review and editing; JF: conceptualization and project design, data curation and formal analysis, review and editing; JDF: conceptualization and project design, data curation and formal analysis, MJF: Resources, conceptualization and project design, training and supervision, critical review, interpretation and editing.

Reference:

1. Zarouchlioti, C., Parfitt, D. A., Li, W., Gittings, L. M. & Cheetham, M. E. DNAJ Proteins in neurodegeneration: Essential and protective factors. *Philosophical Transactions of the Royal Society B: Biological Sciences* **373**, 1–13 (2018).
2. Gorenberg, E. L. & Chandra, S. S. The Role of Co-chaperones in Synaptic Proteostasis and Neurodegenerative Disease. *Front Neurosci* **11**, 1–16 (2017).
3. Van Spronsen, F. J. *et al.* Heterogeneous clinical spectrum of DNAJC12-deficient hyperphenylalaninemia: From attention deficit to severe dystonia and intellectual disability. *J Med Genet* **55**, 249–253 (2018).
4. Anikster, Y. *et al.* Biallelic Mutations in DNAJC12 Cause Hyperphenylalaninemia, Dystonia, and Intellectual Disability. *Am J Hum Genet* **100**, 257–266 (2017).
5. Straniero, L. *et al.* DNAJC12 and dopa-responsive nonprogressive parkinsonism. *Ann Neurol* **82**, 640–646 (2017).
6. Veenma, D., Cordeiro, D., Sondheimer, N. & Mercimek-Andrews, S. DNAJC12-associated developmental delay, movement disorder, and mild hyperphenylalaninemia identified by whole-exome sequencing re-analysis. *European Journal of Human Genetics* **26**, 1867–1870 (2018).
7. Gallego, D. *et al.* Pathogenic variants of DNAJC12 and evaluation of the encoded cochaperone as a genetic modifier of hyperphenylalaninemia. *Hum Mutat* **41**, 1329–1338 (2020).

8. de Sain-van der Velden, M. G. M. *et al.* Beneficial effect of BH4 treatment in a 15-year-old boy with biallelic mutations in DNAJC12. in *JIMD Reports* vol. 42 99–103 (Springer, 2018).

9. Deng, I. B., Follett, J., Bu, M. & Farrer, M. J. DNAJC12 in Monoamine Metabolism, Neurodevelopment, and Neurodegeneration. *Movement Disorders* **39**, 249–258 (2024).

10. van Spronsen, F. J. *et al.* Phenylketonuria. *Nature Reviews Disease Primers* vol. 7 Preprint at https://doi.org/10.1038/s41572-021-00267-0 (2021).

11. Edvardson, S. *et al.* A Deleterious Mutation in DNAJC6 Encoding the Neuronal-Specific Clathrin-Uncoating Co-Chaperone Auxilin, Is Associated with Juvenile Parkinsonism. *PLoS One* **7**, 1–5 (2012).

12. Nalls, M. A. *et al.* Large-scale meta-analysis of genome-wide association data identifies six new risk loci for Parkinson's disease. *Nat Genet* **46**, 989–993 (2014).

13. Nosková, L. *et al.* Mutations in DNAJC5, Encoding Cysteine-String Protein Alpha, Cause Autosomal-Dominant Adult-Onset Neuronal Ceroid Lipofuscinosis. *The American Journal of Human Genetics* **89**, 241–252 (2011).

14. Vilariño-Güell, C. *et al.* DNAJC13 mutations in Parkinson disease. *Hum Mol Genet* **23**, 1794–1801 (2014).

15. Wider, C. *et al.* Study of a Swiss dopa-responsive dystonia family with a deletion in GCH1 *Neurology* **70**, 1377 (2008).

16. Guella, I. *et al.* Parkinsonism in GTP cyclohydrolase 1 mutation carriers. *Brain* **138**, e349–e349 (2015).

17. Guella, I. *et al.* Parkinsonism in GTP cyclohydrolase 1 mutation carriers. *Brain* **138**, 1–2 (2015).

18. Yoshino, H. *et al.* GCH1 mutations in dopa-responsive dystonia and Parkinson's disease. *J Neurol* **265**, 1860–1870 (2018).

19. Mencacci, N. E. *et al.* Parkinson's disease in GTP cyclohydrolase 1 mutation carriers. *Brain* **137**, 2480–2492 (2014).

20. Shetty, A. S., Bhatia, K. P. & Lang, A. E. Dystonia and Parkinson's disease: What is the relationship? *Neurobiol Dis* **132**, 1–10 (2019).

21. Porta, F., Neirotti, A. & Spada, M. Restless legs syndrome in DNAJC12 deficiency. *Neurological Sciences* 1–6 (2023) doi:10.1007/s10072-023-06733-9.

22. Porta, F., Ponzone, A. & Spada, M. Phenylalanine and tyrosine metabolism in DNAJC12 deficiency: A comparison between inherited hyperphenylalaninemias and healthy subjects. *European Journal of Paediatric Neurology* **28**, 77–80 (2020).

23. Cobb, S. A. *et al.* GCH1 in early-onset Parkinson's disease. *Movement Disorders* **24**, 2070–2075 (2009).

24. Opladen, T. *et al.* Clinical and biochemical characterization of patients with early infantile onset of autosomal recessive GTP cyclohydrolase I deficiency without hyperphenylalaninemia. *Movement Disorders* **26**, 157–161 (2011).

25. AU - Tatem, K. S. *et al.* Behavioral and Locomotor Measurements Using an Open Field Activity Monitoring System for Skeletal Muscle Diseases. *JoVE* e51785 (2014) doi:doi:10.3791/51785.

26. Takeshita, H. *et al.* Modified forelimb grip strength test detects aging-associated physiological decline in skeletal muscle function in male mice. *Sci Rep* **7**, 42323 (2017).

27. Luong, T. N., Carlisle, H. J., Southwell, A. & Patterson, P. H. Assessment of Motor Balance and Coordination in Mice using the Balance Beam. *JoVE* e2376 (2011) doi:doi:10.3791/2376.

28. Liu, Y. *et al.* Alteration of the cholinergic system and motor deficits in cholinergic neuron-specific Dyt1 knockout mice. *Neurobiol Dis* **154**, 105342 (2021).

29. Cataldi, S. *et al.* Altered dopamine release and monoamine transporters in Vps35 p.D620N knock-in mice. *NPJ Parkinsons Dis* **4**, 27 (2018).

30. Bu, M. *et al.* Inhibition of LRRK2 kinase activity rescues deficits in striatal dopamine physiology in VPS35 p.D620N knock-in mice. *NPJ Parkinsons Dis* **9**, 167 (2023).

31. Gustavsson, E. K. *et al.* RAB32 Ser71Arg in autosomal dominant Parkinson's disease: linkage, association, and functional analyses. *Lancet Neurol* **23**, 603–614 (2024).

32. Cataldi, S. *et al.* Altered dopamine release and monoamine transporters in Vps35 p.D620N knock-in mice. *NPJ Parkinsons Dis* **4**, 27 (2018).

33. Volta, M. *et al.* Initial elevations in glutamate and dopamine neurotransmission decline with age, as does exploratory behavior, in LRRK2 G2019S knock-in mice. *Elife* **6**, e28377 (2017).

34. Martinez, A. *et al.* Structural recognition and stabilization of tyrosine hydroxylase by the J-domain protein DNAJC12. (2023) doi:10.21203/rs.3.rs-3621320/v1.

35. Parra, L. A. *et al.* The molecular chaperone Hsc70 interacts with tyrosine hydroxylase to regulate enzyme activity and synaptic vesicle localization. *Journal of Biological Chemistry* **291**, 17510–17522 (2016).

36. Requena, D. F. *et al.* The molecular chaperone Hsc70 interacts with the vesicular monoamine transporter-2. *J Neurochem* **110**, 581–594 (2009).

37. Ichimura, T., Isobe, T., Okuyama, T., Yamauchi, T. & Fujisawa, H. Brain 14-3-3 protein is an activator protein that activates tryptophan 5-monooxygenase and tyrosine 3-monooxygenase in the presence of Ca2+,calmodulin-dependent protein kinase II. *FEBS Lett* **219**, 79–82 (1987).

38. Matsuda, W. *et al.* Single Nigrostriatal Dopaminergic Neurons Form Widely Spread and Highly Dense Axonal Arborizations in the Neostriatum. *The Journal of Neuroscience* **29**, 444 (2009).

39. Choi, J., Djebbar, S., Fournier, A. & Labrie, C. The co-chaperone DNAJC12 binds to Hsc70 and is upregulated by endoplasmic reticulum stress. *Cell Stress Chaperones* **19**, 439–446 (2014).

40. Klein, M. O. *et al.* Dopamine: Functions, Signaling, and Association with Neurological Diseases. *Cell Mol Neurobiol* **39**, 31–59 (2019).

41. Hikosaka, O., Nakamura, K., Sakai, K. & Nakahara, H. Central mechanisms of motor skill learning. *Curr Opin Neurobiol* **12**, 217–222 (2002).

42. Wise, R. A. Roles for nigrostriatal—not just mesocorticolimbic—dopamine in reward and addiction. *Trends Neurosci* **32**, 517–524 (2009).

43. Li, M. *et al.* Two novel mutations in DNAJC12 identified by whole-exome sequencing in a patient with mild hyperphenylalaninemia. *Mol Genet Genomic Med* **8**, 1–6 (2020).

44. Feng, Y. *et al.* Identification of an inherited pathogenic DNAJC12 variant in a patient with hyperphenylalalinemia. *Clinica Chimica Acta* **490**, 172–175 (2019).

45. Dunkley, P. R. & Dickson, P. W. Tyrosine hydroxylase phosphorylation in vivo. *Journal of Neurochemistry* vol. 149 706–728 Preprint at https://doi.org/10.1111/jnc.14675 (2019).

46. Nagatsu, T. & Nagatsu, I. Tyrosine hydroxylase (TH), its cofactor tetrahydrobiopterin (BH4), other catecholamine-related enzymes, and their human genes in relation to the drug and gene therapies of Parkinson's disease (PD): historical overview and future prospects. *J Neural Transm* **123**, 1255–1278 (2016).

47. Nagatsu, T., Nakashima, A., Ichinose, H. & Kobayashi, K. Human tyrosine hydroxylase in Parkinson's disease and in related disorders. *J Neural Transm* **126**, 397–409 (2019).

48. Rausch, W.-D., Wang, F. & Radad, K. From the tyrosine hydroxylase hypothesis of Parkinson's disease to modern strategies: a short historical overview. *J Neural Transm* **129**, 487–495 (2022).

49. Thöny, B. *et al.* Tetrahydrobiopterin shows chaperone activity for tyrosine hydroxylase. *J Neurochem* **106**, 672–681 (2008).

50. Nagatsu, T. & Sawada, M. Biochemistry of postmortem brains in Parkinson's disease: historical overview and future prospects. in *Neuropsychiatric Disorders An Integrative Approach* (eds. Gerlach, M., Deckert, J., Double, K. & Koutsilieri, E.) 113–120 (Springer Vienna, Vienna, 2007).

51. Choi, H. J., Jang, Y. J., Kim, H. J. & Hwang, O. Tetrahydrobiopterin Is Released from and Causes Preferential Death of Catecholaminergic Cells by Oxidative Stress. *Mol Pharmacol* **58**, 633 (2000).

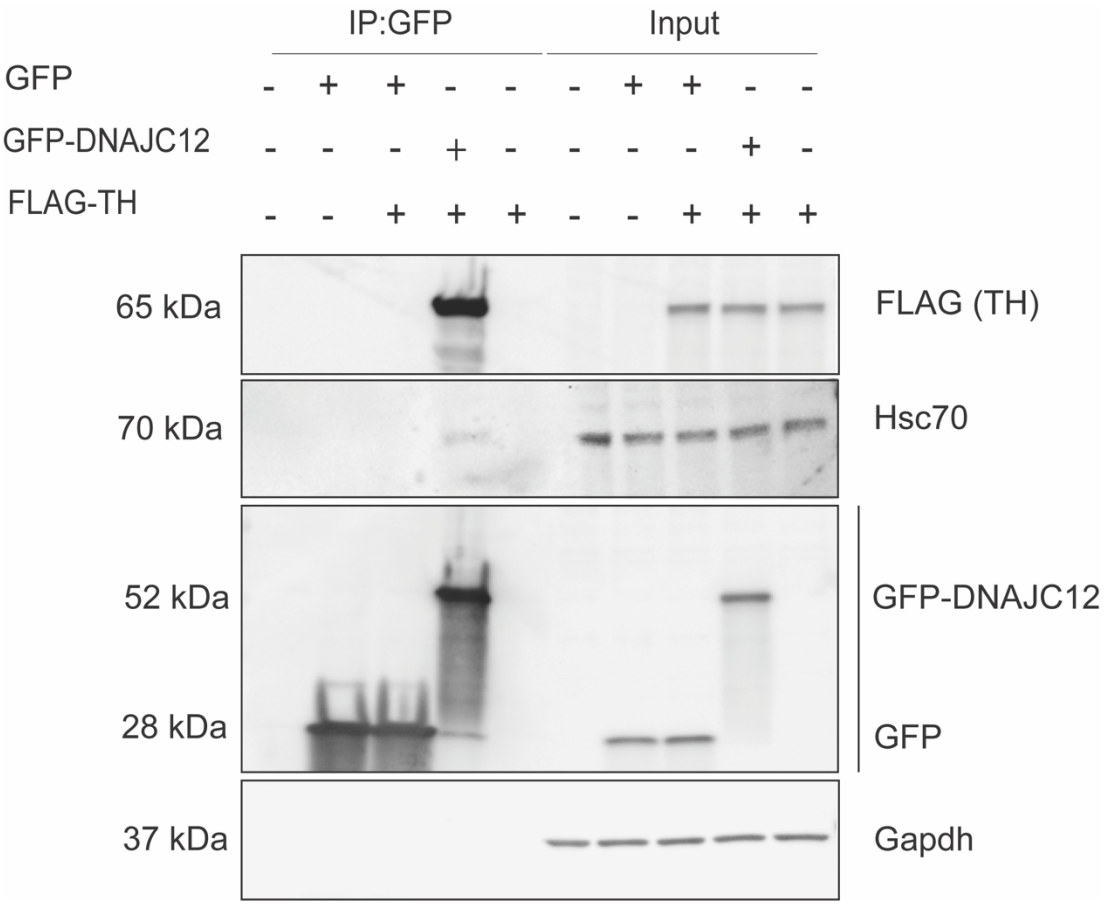
IP:GFP
Input
GFP
- + + - - - + + - -
GFP-DNAJC12
- - - + - - - - + -
FLAG-TH
- - + + + - - + + +
65 kDa
FLAG (TH)
70 kDa
Hsc70
52 kDa
GFP-DNAJC12
28 kDa
GFP
37 kDa
Gapdh

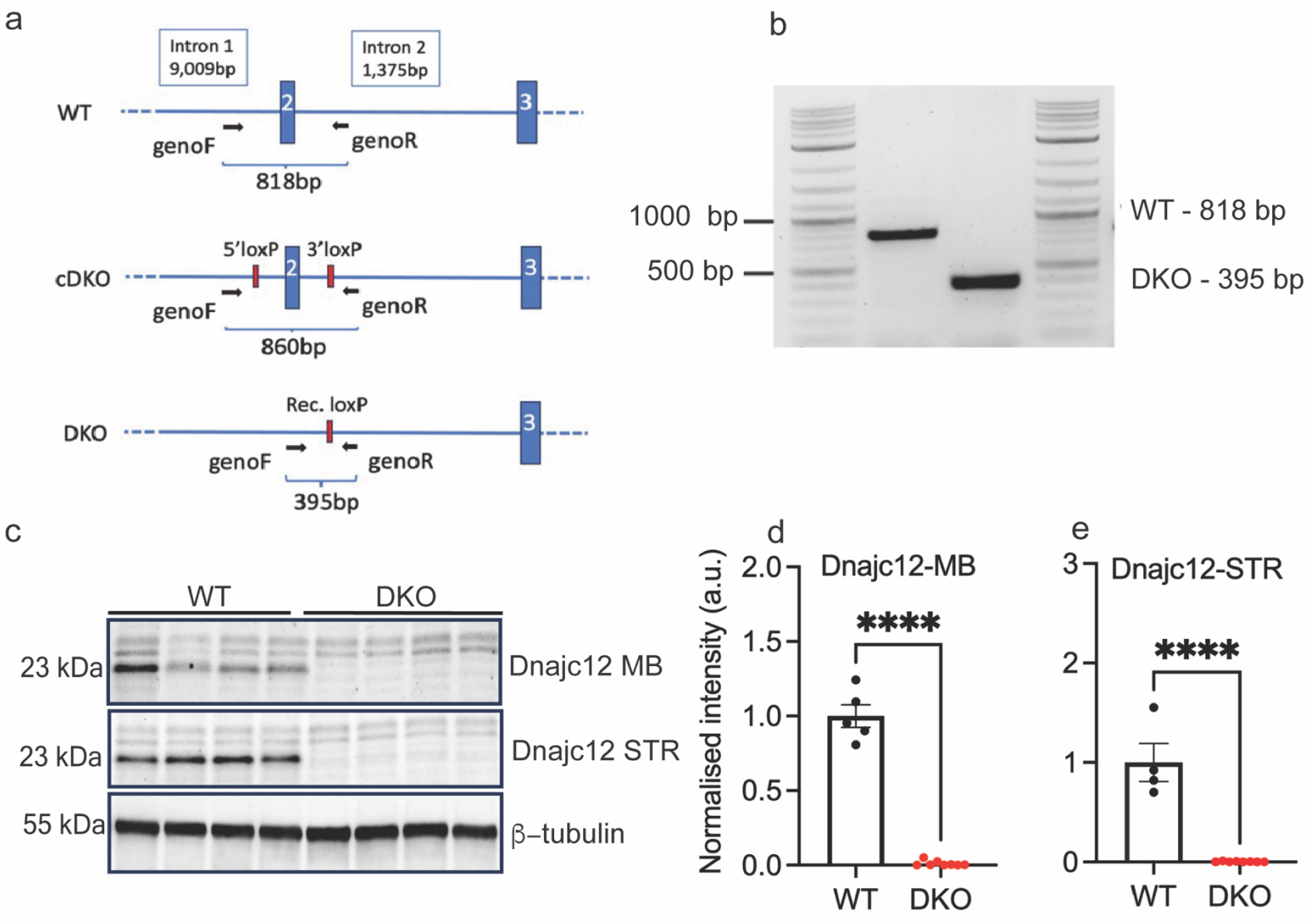
a
Intron 1
9,009bp
Intron 2
1,375bp
WT
2
3
genoF
genoR
818bp
5'loxP
3'loxP
cDKO
860bp
Rec. loxP
DKO
395bp
b
1000 bp
500 bp
WT - 818 bp
DKO - 395 bp
c
WT
DKO
23 kDa
Dnajc12 MB
23 kDa
Dnajc12 STR
55 kDa
β–tubulin
d
Dnajc12-MB
Normalised intensity (a.u.)
2.0
1.5
1.0
0.5
0.0
****
WT
DKO
e
Dnajc12-STR
3
2
1
0
****
WT
DKO

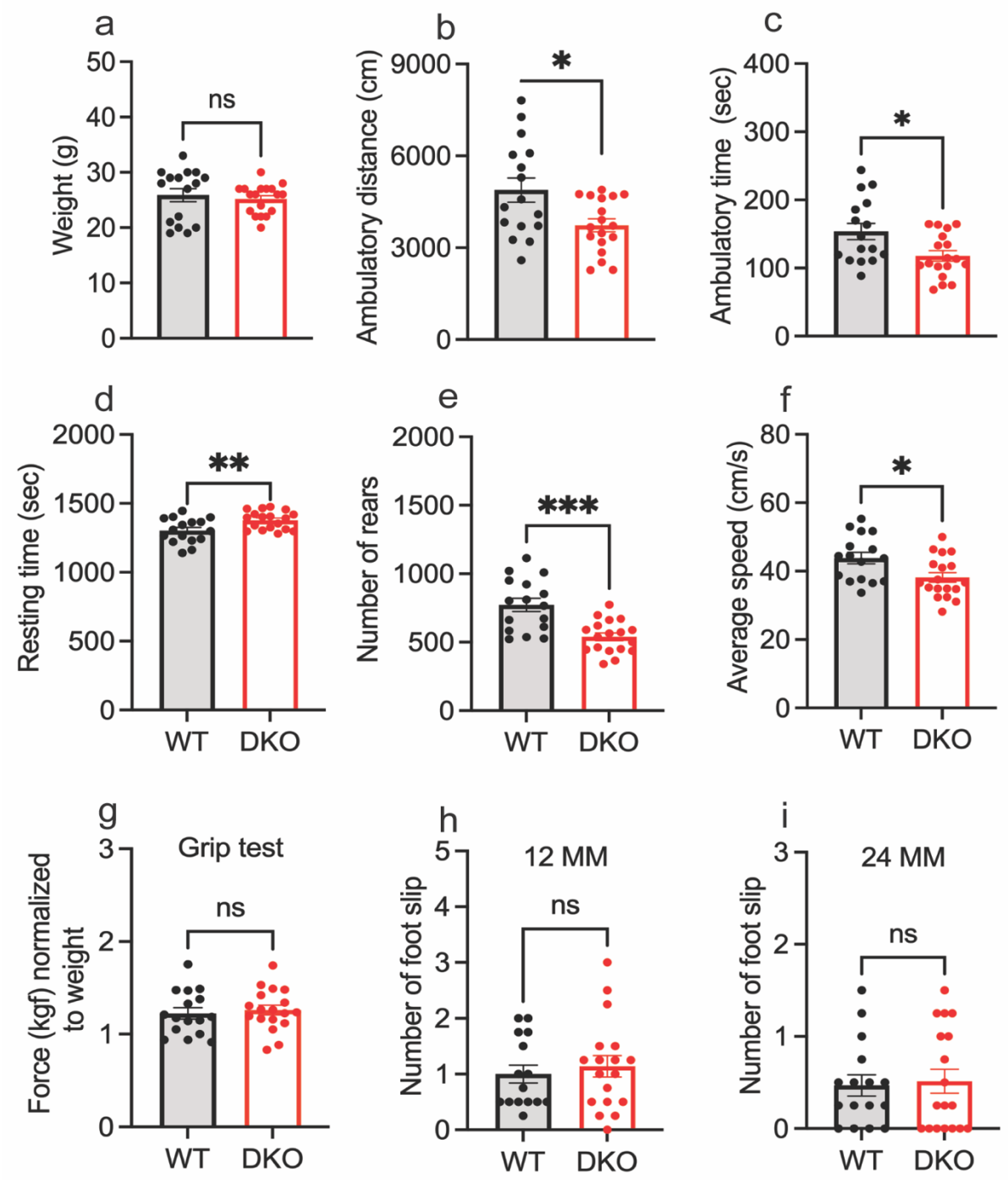
a
Weight (g)
50
40
30
20
10
0
ns
b
Ambulatory distance (cm)
9000
6000
3000
0
*
c
Ambulatory time (sec)
400
300
200
100
0
*
d
Resting time (sec)
2000
1500
1000
500
0
**
WT
DKO
e
Number of rears
2000
1500
1000
500
0
***
WT
DKO
f
Average speed (cm/s)
80
60
40
20
0
*
WT
DKO
g
Grip test
Force (kgf) normalized to weight
3
2
1
0
ns
WT
DKO
h
12 MM
Number of foot slip
5
4
3
2
1
0
ns
WT
DKO
i
24 MM
Number of foot slip
3
2
1
0
ns
WT
DKO

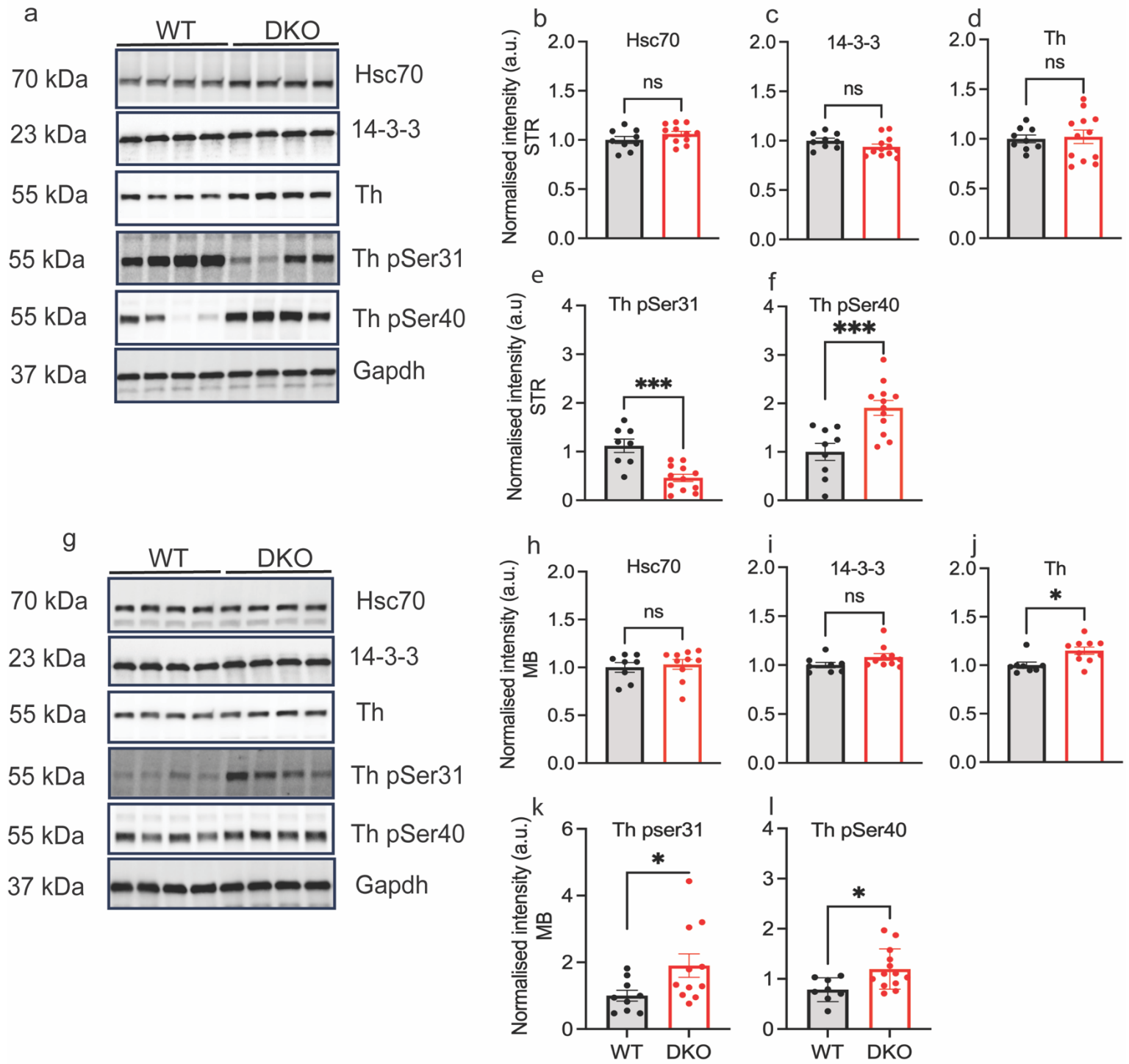
a
WT
DKO
70 kDa
Hsc70
23 kDa
14-3-3
55 kDa
Th
55 kDa
Th pSer31
55 kDa
Th pSer40
37 kDa
Gapdh
b
Hsc70
ns
c
14-3-3
ns
d
Th
ns
Normalised intensity (a.u.)
STR
e
Th pSer31
***
f
Th pSer40
***
g
WT
DKO
70 kDa
Hsc70
23 kDa
14-3-3
55 kDa
Th
55 kDa
Th pSer31
55 kDa
Th pSer40
37 kDa
Gapdh
h
Hsc70
ns
i
14-3-3
ns
j
Th
*
Normalised intensity (a.u.)
MB
k
Th pser31
*
l
Th pSer40
*
WT
DKO

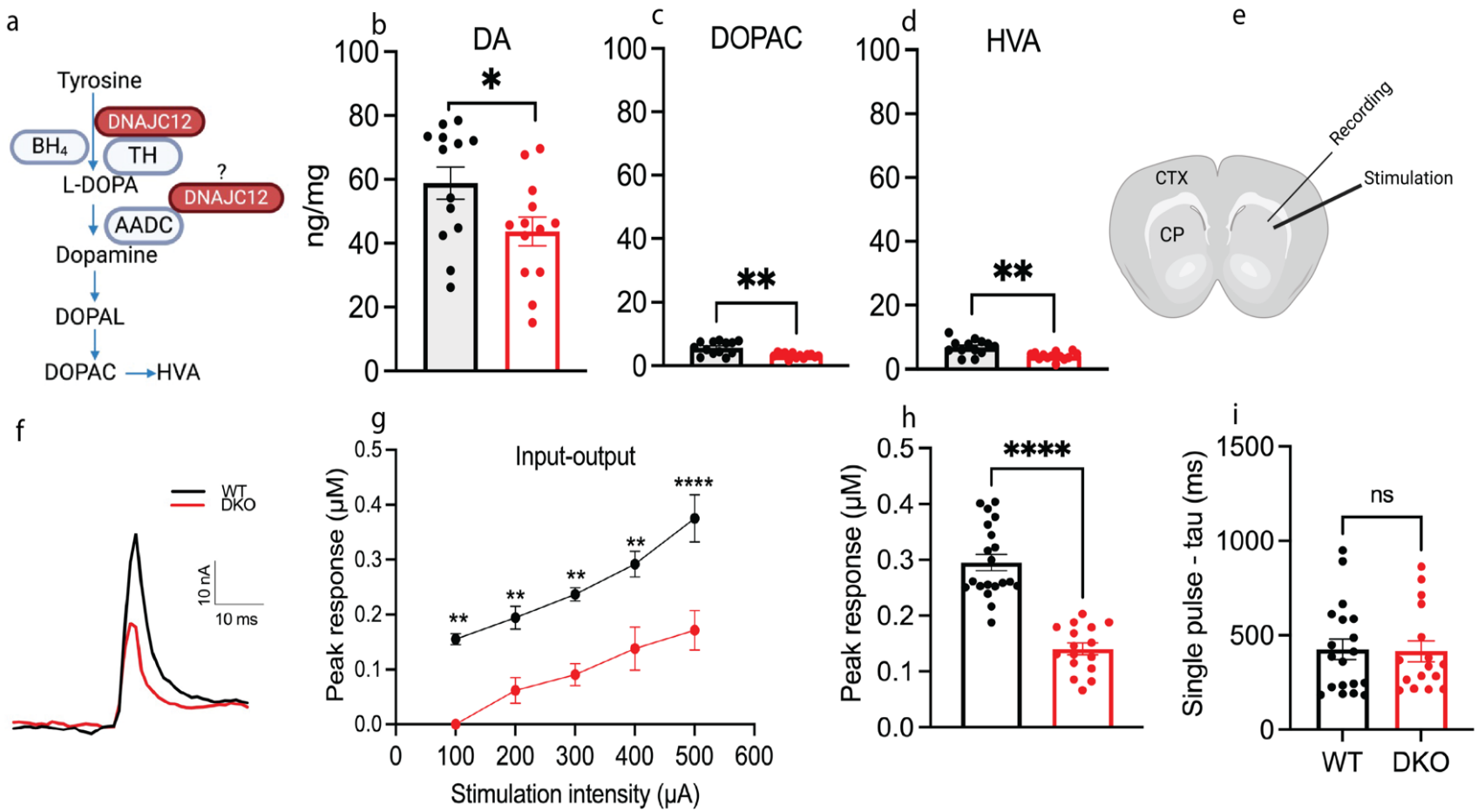
a
Tyrosine
DNAJC12
BH4
TH
?
L-DOPA
DNAJC12
AADC
Dopamine
DOPAL
DOPAC
HVA
b
DA
ng/mg
*
c
DOPAC
**
d
HVA
**
e
Recording
Stimulation
CTX
CP
f
WT
DKO
10 nA
10 ms
g
Input-output
Peak response (μM)
Stimulation intensity (μA)
**
****
h
Peak response (μM)
****
i
Single pulse - tau (ms)
ns
WT
DKO

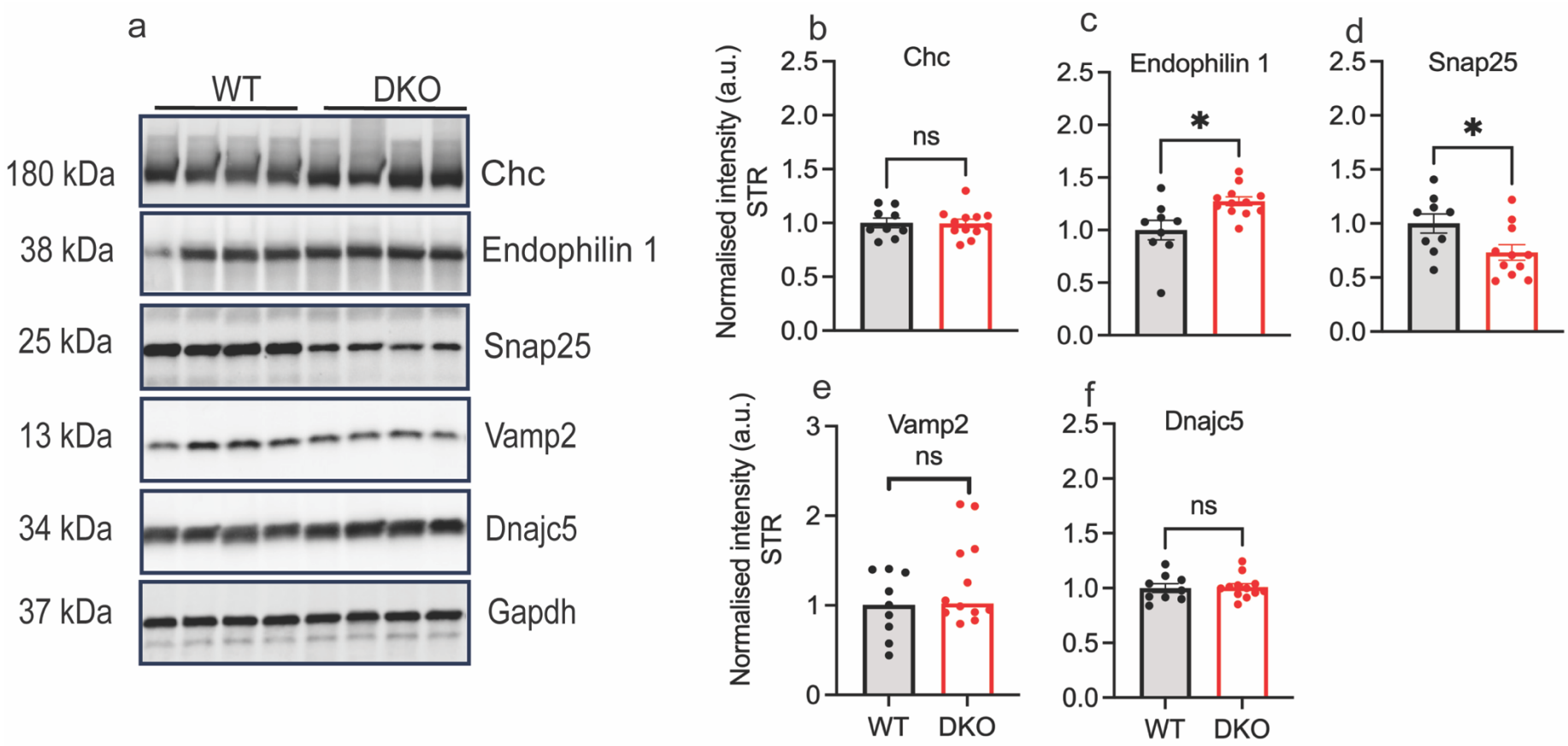
a
WT
DKO
180 kDa
Chc
38 kDa
Endophilin 1
25 kDa
Snap25
13 kDa
Vamp2
34 kDa
Dnajc5
37 kDa
Gapdh
b
Chc
ns
c
Endophilin 1
*
d
Snap25
*
e
Vamp2
ns
f
Dnajc5
ns
Normalised intensity (a.u.)
STR
WT
DKO

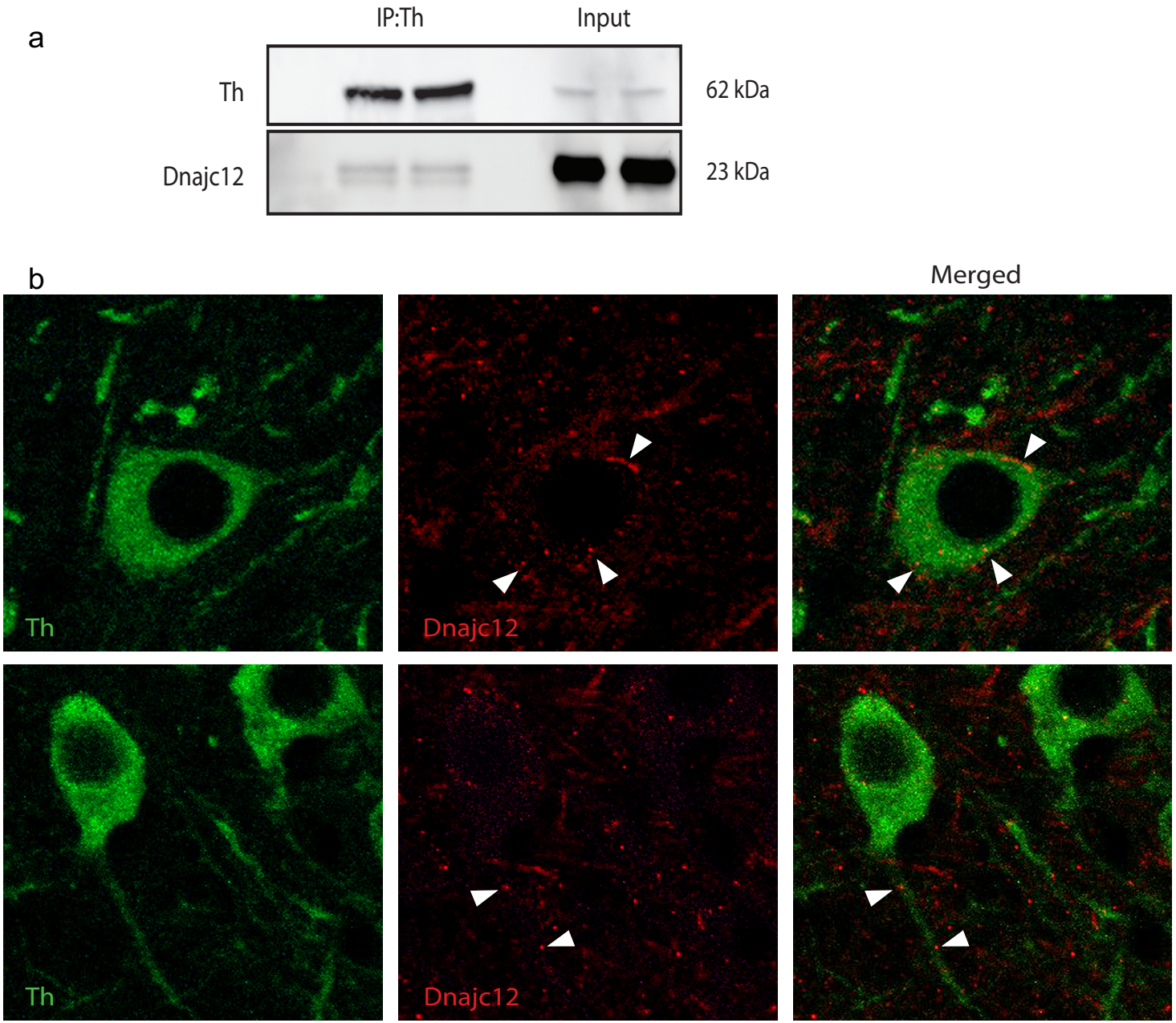
a
IP:Th
Input
Th
62 kDa
Dnajc12
23 kDa
b
Merged
Th
Dnajc12
Th
Dnajc12

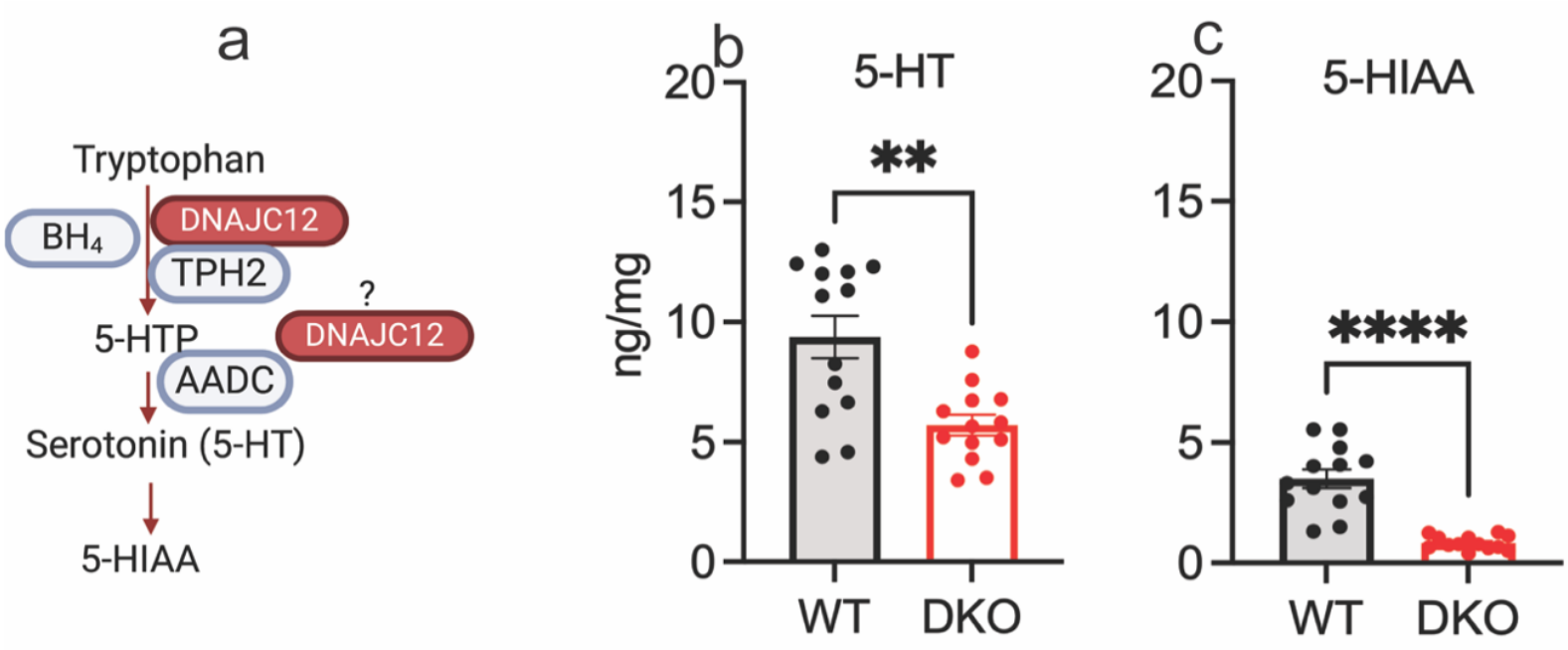
a
Tryptophan
BH4
DNAJC12
TPH2
?
5-HTP
DNAJC12
AADC
Serotonin (5-HT)
5-HIAA
b
5-HT
ng/mg
20
15
10
5
0
**
WT
DKO
c
5-HIAA
20
15
10
5
0
****
WT
DKO

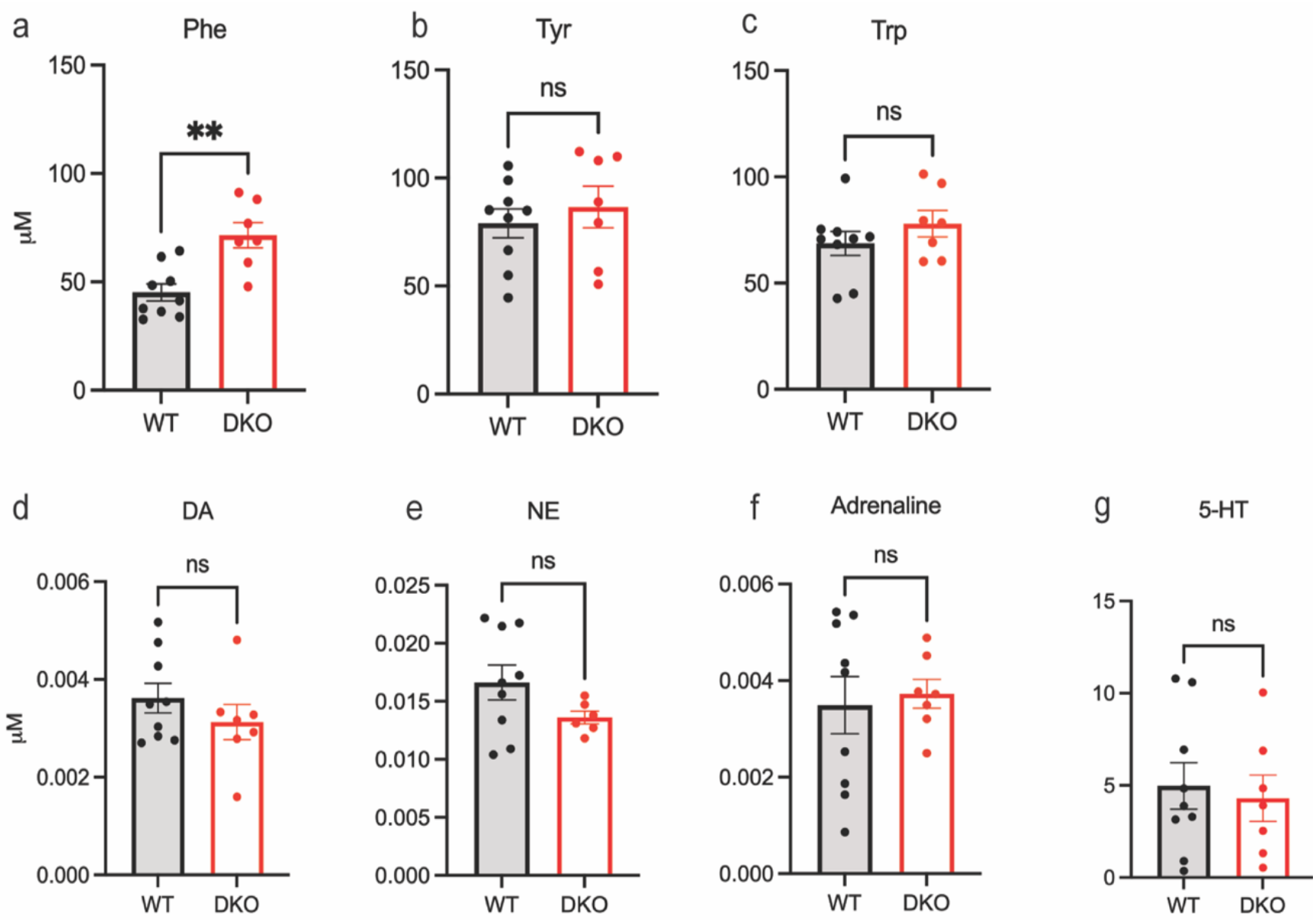
a
Phe
150
100
50
0
μM
**
WT
DKO
b
Tyr
150
100
50
0
ns
WT
DKO
c
Trp
150
100
50
0
ns
WT
DKO
d
DA
0.006
0.004
0.002
0.000
μM
ns
WT
DKO
e
NE
0.025
0.020
0.015
0.010
0.005
0.000
ns
WT
DKO
f
Adrenaline
0.006
0.004
0.002
0.000
ns
WT
DKO
g
5-HT
15
10
5
0
ns
WT
DKO

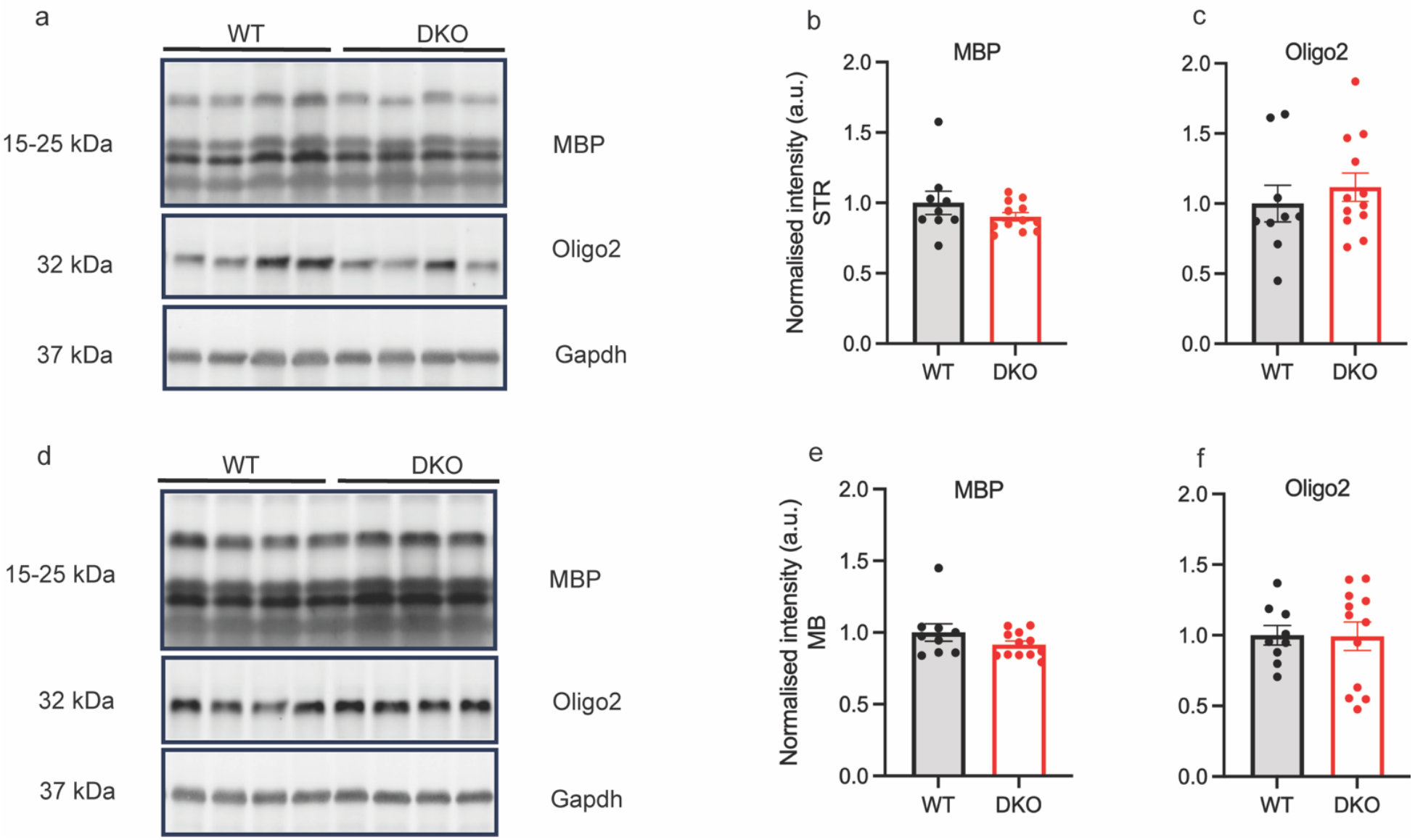
a
WT
DKO
15-25 kDa
MBP
32 kDa
Oligo2
37 kDa
Gapdh
b
MBP
Normalised intensity (a.u.)
STR
2.0
1.5
1.0
0.5
0.0
WT
DKO
c
Oligo2
2.0
1.5
1.0
0.5
0.0
WT
DKO
d
WT
DKO
15-25 kDa
MBP
32 kDa
Oligo2
37 kDa
Gapdh
e
MBP
Normalised intensity (a.u.)
MB
2.0
1.5
1.0
0.5
0.0
WT
DKO
f
Oligo2
2.0
1.5
1.0
0.5
0.0
WT
DKO